Design and Evaluation of a New Body for Falling Cylinder Viscometers

JOHN LOHRENZ and FRED KURATA

The University of Kansas, Lawrence, Kansas

A new body with stabilizers removed from the cylindrical section was designed for falling cylinder viscometers. Experimental data to evaluate the new body were obtained with gases and liquids at varying temperatures and pressures.

Experimental results showed improved agreement with a theoretical model that assumes laminar flow friction along the cylindrical portion of the body and negligible additional frictional effects. Effects of temperature and pressure were accurately predicted by this theoretical model. The data were correlated on an improved viscometer plot.

The advantage of the new body design was a negligible frictional effect of the stabilizers. The entrance-exit frictional effect was evaluated from the experimental data and correlated on a friction factor plot. Fluid flow in the annulus remained laminar throughout this study. The results of this investigation allow an improved prediction of the falling-cylinder viscometer constant.

For falling body viscometers a viscometer constant β may be defined as follows:

$$\beta = \frac{\mu v}{(\sigma - \rho)} \qquad (1)$$

This viscometer constant is a function of both the dimensions of the viscometer and the type of flow regime. The value of β is constant at different values of v, σ, ρ, and μ only if the dimensions of the viscometer are constant and all flow is laminar.

For falling cylinder viscometers Lohrenz, Swift, and Kurata (7) derived a viscometer constant β_{lsf} as follows:

$$\beta_{lsf} = \frac{D_e^2 g l'}{16\, l} \qquad (2)$$

The two viscometer constants β and β_{lsf} are equal only in the case of laminar flow in the annulus between the falling cylinder and the viscometer tube and negligible additional frictional effects.

Although β was approximated by β_{lsf} in the laminar region, Lohrenz, Swift, and Kurata (7) found predicted values of β_{lsf} were higher than experimental values of β over the whole range of Reynolds numbers owing to the presence of frictional effects not considered in the derivation of Equation (2). The additional effects were friction caused by entrance and exit of the fluid in and from the annulus, and friction from flow past the stabilizers used to reduce flutter of the falling cylindrical body.

From knowledge of the thermal expansion of the materials of construction of the viscometer Lohrenz, Swift, and Kurata (7) found the model used in Equation (2) gave an accurate prediction of the effect of temperature on the viscometer constant. They showed that the function of β/β_{lsf} vs. N_{Re} would give a valid calibration plot. No advantage of precision for this plot over the conventional Sage and Lacey (11) type of plot of $\beta_{0,0}$ vs. $v\rho/\mu$ was found however.

John Lohrenz is with the Continental Oil Company, Ponca City, Oklahoma.

DESIGN OF A NEW FALLING BODY

Swift (12) used falling bodies with stabilizers projecting from the cylindrical portion to prevent flutter. Much of the additional friction not considered in Equation (2) was caused by the fluid flowing around the stabilizers at high velocity in the annulus of the viscometer. A new falling cylindrical body was designed with the following two requirements: The stabilizers which are necessary for reproducible data should cause little or negligible friction, and the additional frictional effects should be separated and evacuated.

The resulting falling cylindrical body is schematically represented on Figure 1. The stabilizers were placed on stems above and below the cylindrical portion of the body. During descent of the body the velocity of the fluid around the stabilizers will be less than in the annulus of the viscometer. Thus the effect of friction on the stabilizers should be correspondingly reduced. The considerations in designing the stabilizer were as follows:

1. The stabilizer should be as small as possible to minimize surface and shape friction.
2. The stabilizer should be sufficiently large to reduce flutter.

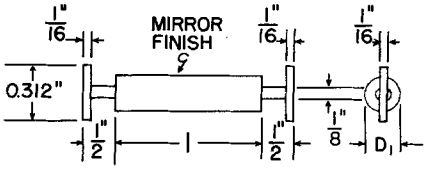

Fig. 1. Schematic drawing of the new falling cylindrical body.

3. The stabilizer must be of simple design so that reasonably uniform stabilizers can be machined on different bodies.

These considerations point in inconsistent directions. The final stabilizer design represented a compromise between these considerations. Initially a four-finned stabilizer similar to the final design was tested. The results were reproducible, indicating no flutter or lack of symmetry. In order to further minimize stabilizer friction the two-finned stabilizer was tested. The good results with this stabilizer led to its selection.

The friction forces acting on the type of body represented on Figure 1 are due to three effects:

1. Flow along the cylindrical portion of the body.
2. Flow of fluid at the entrance and exit of the annulus.
3. Flow past the stabilizers.

The forces due to these three frictional effects are balanced by the force of gravity when the body is falling at the terminal velocity. By dimensional analysis

$$f_c = \frac{4F_c g_c D_e}{\pi D_1^2 \rho v^2 l} = \phi_1(N_{Re}, D_1/D_e) \qquad (3)$$

and

$$f_{ee} = \frac{4F_{ee} g_c}{\pi D_1^2 \rho v^2} = \phi_2(N_{Re}, D_1/D_e) \qquad (4)$$

When one considers a stabilizer of given dimensions, the dimensional function

$$f_{st} = \frac{F_{st}}{\rho v^2} = \phi_3\,(v\rho/\mu) \qquad (5)$$

may be written. Equating forces and rearranging one obtains

$$f = f_c + \frac{f_{ee} D_e}{l} + \frac{4 f_{st} g_c D_e}{\pi D_1^2 l} \qquad (6)$$

where f is the total friction factor previously defined by Lohrenz, Swift, and Kurata (7). In Equation (6) each of the terms on the right is proportional to the magnitude of the friction of the cylindrical portion of the body, that caused by the entrance-exit effect, and that caused by the stabilizer, respectively.

When one assumes that different frictional effects do not interact and

TABLE 1. PROPERTIES OF THE VISCOMETER TUBE AND THE FALLING CYLINDRICAL BODIES

Internal diameter of the viscometer tube = D_1 = 0.3149 in.
Density of the falling cylindrical bodies = σ = 1.7832 g./cc.

Body code	Diameter of the cylindrical section of the body D_1, (in.)	Length of the cylindrical section of the body l, (in.)	Volume equivalent length, l',* (in.)
L-308	0.3079	3.000	3.183
L-304	0.3038	3.000	3.182
L-300	0.2997	3.000	3.201
L-296	0.2960	3.000	3.194
M-308	0.3079	2.000	2.184
M-304	0.3040	2.000	2.185
M-300	0.3000	2.000	2.187
M-296	0.2960	2.000	2.196
S-308	0.3078	1.000	1.188
S-304	0.3035	1.000	1.175
S-300	0.2998	1.000	1.211
S-296	0.2962	1.000	1.203

* Computed as $l' = 4V/\pi D_1^2$. The volume equivalent length l' is equal to the length of a right cylinder of diameter D_1 having a volume equal to the body.

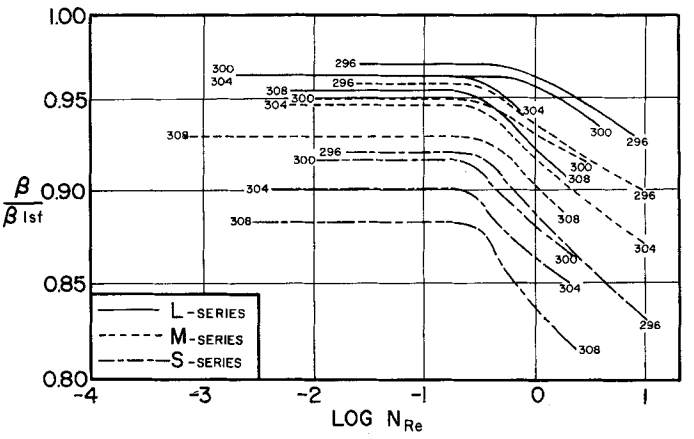

Fig. 2. β/β_{1sf} vs. N_{Re} for the twelve falling cylindrical bodies.

are separable, the stabilizer friction factor f_{st} may be experimentally determined as a function of $v\rho/\mu$ using a body made up only of the stabilizer. While the assumption of noninteraction and separation of frictional effects may not be absolutely valid for a comparatively small stabilizer frictional effect, this assumption should reasonably apply. If f_{st} is known, Equation (6) may be solved for f_e and f_{ee} if two experimental values of f for bodies of different length l are available at a constant N_{Re} and D_1/D_e. Equation (6) may be used in this manner to separate and evaluate the different frictional effects with the inherent assumption that the various effects do not interact.

EXPERIMENTAL APPARATUS, PROCEDURE, AND RESULTS

Twelve new magnesium falling cylindrical bodies were constructed. The length l and the ratio D_1/D_e were systematically varied. Each body had a stabilizer of the dimensions shown on Figure 1. The properties of the bodies and the viscometer tube are shown on Table 1. A magnesium body consisting only of the stabilizer was also constructed. The viscometer constants did not vary with time. The finish on the bodies did not change with use in hydrocarbons and dry nitrogen.

The experimental apparatus has been described by Swift and others (*12, 13*). The modifications of the experimental procedure of Swift (*12*) are given by Lohrenz (*6*).

The terminal velocities of the bodies were determined in various fluids. The temperature range was —100° to 100°C. The standard deviation for errors in temperature control and measurement was ±0.013°C. Pressures were as high as 600 lb./sq.in. Both gas and liquid fluids were used. *N*-pentane, *n*-hexane, *n*-heptane, *n*-octane, and *n*-decane below the normal boiling point were used as saturated and subcooled liquids. Sources of liquid viscosity and density data were Rossini (*10*) and Bridgman (*1, 2*). Gaseous nitrogen at 1 atm. and under pressure was used. Viscosity and density data for nitrogen were taken from Hilsenrath et al. (*3*), Kestin and Wang (*5*), Michels and Gibson (*8*), Ross and Brown (*9*), and Ross and Hanks (*4*). Estimated accuracy of the viscosity and density data used was better than 1%.

Terminal velocities ranged from 30 to 0.01 cm./sec. for a viscosity range from 3 to 0.01 centipoise. Detailed experimental results were given by Lohrenz (*6*).*

For the range of $v\rho/\mu$ obtained for the twelve falling cylindrical bodies, terminal velocities of the stabilizer body were obtained with *n*-decane and standard viscosity oils from the National Bureau of Standards as fluids.

* Complete experimental data and calculations have been deposited as document 7083 with the American Documentation Institute, Photoduplication Service, Library of Congress, Washington 25, D. C., and may be obtained for $5.00 for photoprints or for $2.25 for 35-mm. microfilm.

TABLE 2. EXPERIMENTAL VISCOMETER CONSTANTS

Body code	β^*/β_{1sf}	$\beta_{(0,0)}(10^4)$,* cc./sec.²
L-308	0.9576	3.093
L-304	0.9653	12.02
L-300	0.9653	29.99
L-296	0.9705	57.57
M-308	0.9321	3.094
M-304	0.9492	11.57
M-300	0.0527	28.81
M-296	0.9608	58.87
S-308	0.8847	3.326
S-304	0.9021	13.39
S-300	0.9188	31.39
S-296	0.9227	60.03

* In the laminar region.

ANALYSIS OF RESULTS

The variation of D_1 and D_2 with temperature and pressure may be computed from the linear coefficient of thermal expansion, Young's modulus, and the Poisson ratio for the materials of construction of the falling cylinder viscometer. End effects which cause a slightly noncylindrical body were neglected. Values of D_1 and D_2 computed in this manner were used to calculate D_e and β_{1sf} as a function of temperature and pressure by Equation (2).

The experimental data were used to plot β/β_{1sf} vs. N_{Re}. The resulting curves for the twelve falling cylindrical bodies are shown on Figure 2. At low values of N_{Re}, β/β_{1sf} was constant, indicating laminar flow. Values of β/β_{1sf} in the laminar region given in Table 2 were consistently higher than the results of Lohrenz, Swift, Kurata (*7*). This corroborated the reasoning which led to the design of the new falling cylindrical body. Values of β/β_{1sf} were consistently higher for bodies of greater length and smaller diameter. This is consistent with the expected decrease in the frictional effects not considered in the derivation of β_{1sf}. Above an N_{Re} of about 0.2, β/β_{1sf} decreased owing to turbulence. Precision of the data for each falling cylindrical body as the per cent standard deviation based on the best curve through the data was about ± 0.6%.

With the data in the laminar region where N_{Re} was less than 0.2, $\beta_{(0,0)}$ and the coefficients of temperature and pressure on the viscometer constant were determined by the method of least squares from experimental values of $\beta_{(t,p)}$ in the following equation:

$$\beta_{(t,p)} = \beta_{(0,0)}(1 + \alpha t)(1 + \gamma p) \qquad (7)$$

Table 2 includes the results. For some of the smaller falling cylindrical bodies determination of the pressure coeffi-

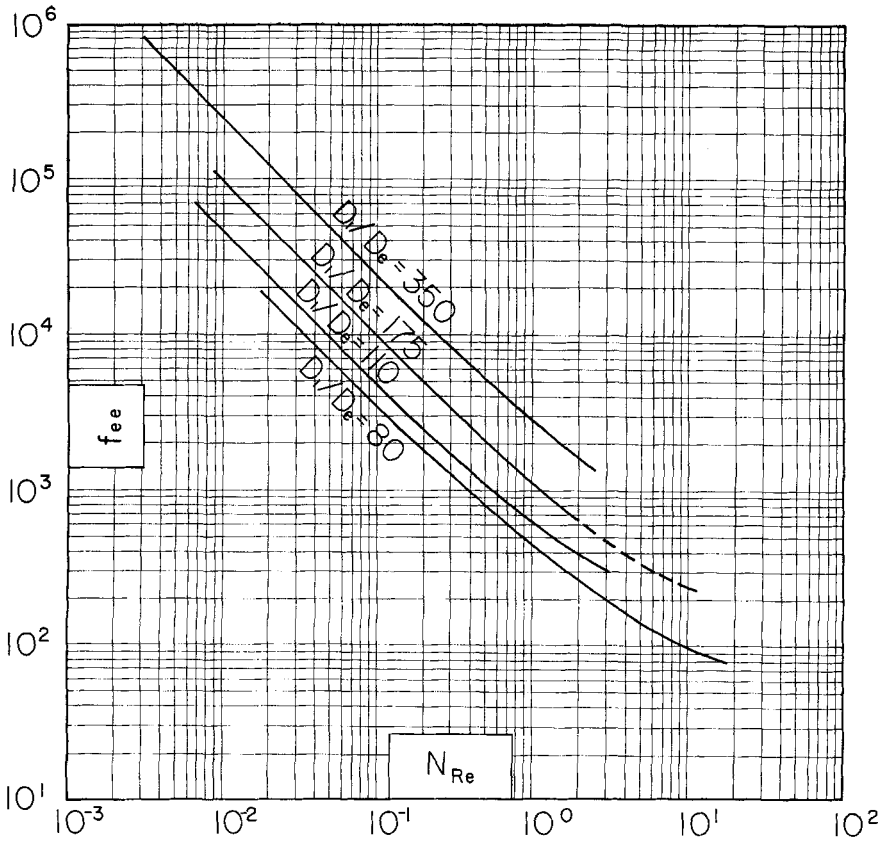

Fig. 3. Correlation of entrance-exit friction.

cient γ was impossible because data for fluids under pressure were not available in the laminar region.

Predicted values of α and γ were calculated on the assumption of independent, linear variation of β_{1sf} with temperature and pressure. Errors in β_{1sf} due to departure from this assumption were a maximum of 1.2%. Average deviation between predicted and experimental temperature coefficients was 5%. The viscometer constant changes as much as 60% between the extremes of the temperature range. The maximum effect of pressure on the viscometer constant was about 3%. The results indicate that effects of temperature and pressure may be accurately predicted by Equation (2).

Sage and Lacey (*11*) type of plots of $\beta_{(0,0)}$ vs. $v\rho/\mu$ were prepared for each falling cylindrical body. Experimental values of $\beta_{(t,p)}$, α, and γ were used to calculate values of $\beta_{(0,0)}$ by Equation (7). The average standard deviation of the data compared with the best curves of $\beta_{(0,0)}$ vs. $v\rho/\mu$ was 0.93%. Comparison with the precision obtained with the β/β_{1sf} vs. N_{Re} plots demonstrated that the latter function is superior.

Values of the total friction factor were calculated as a function of N_{Re} with values of β/β_{1sf} from Figure 2 in the following relation:

$$f = \frac{16\beta_{1sf}}{N_{Re}\beta} \qquad (8)$$

The stabilizer friction factor f_{st} was calculated as a function of $v\rho/\mu$ with the data obtained with the stabilizer body. The stabilizer friction term in Equation (6), $\dfrac{4f_{st}\,g_c\,D_e}{\pi D_1^2\,l}$, with f_{st} at a value of $v\rho/\mu$ equivalent to N_{Re}, was always insignificant compared with the total friction factor. This established that the stabilizer contributed negligible friction.

Equation (6) was solved for f_c and f_{ee} as a function of N_{Re} and D_1/D_e in accordance with the procedure designed for this study. Figure 3 shows the resulting correlation for f_{ee}. The cylinder friction factor f_c was not a function of D_1/D_e. The function of f_c vs. N_{Re} was given by

$$f_c = \frac{16}{N_{Re}} \qquad (9)$$

The deviation of f_c in this study never exceeded 3%. This means that the flow in the annulus along the cylindrical portion of the body was laminar up to a Reynolds number of at least 10. The 3% maximum deviation was consistent with a possible error of 0.0001 in. in measurement of D_1 and D_2.

CONCLUSIONS

1. A new falling cylindrical body was designed with the advantage of less frictional effects other than along the cylindrical portion of the body.

2. Equation (2) may be used to predict the effects of temperature and pressure on the viscometer constant.

3. The plot of β/β_{1sf} vs. N_{Re} represents calibration data for falling cylinder viscometers with better precision than the $\beta_{(0,0)}$ vs. $v\rho/\mu$ plot.

4. Flutter of falling cylindrical bodies may be prevented with stabilizers which contribute negligible friction.

5. The flow in the annulus of falling cylinder viscometers is laminar up to a Reynolds number of at least 10.

6. Falling cylinder viscometers may be designed or operated without calibration with an accuracy of 3% with a stabilizer which causes negligible friction, Equation (2) to predict the friction on the cylindrical portion of the body, and Figure 3 to predict the entrance and exit friction.

ACKNOWLEDGMENT

The Phillips Petroleum Company furnished financial assistance for this study and donated the hydrocarbons used.

NOTATION

D_1 = diameter of the cylindrical portion of the viscometer body, cm.

D_2 = internal diameter of the viscometer tube, cm.

$D_e = D_1\sqrt{2\{\ln(D_2/D_1) - [(D_2^2 - D_1^2)/(D_2^2 + D_1^2)]\}}$ = equivalent diameter of the viscometer annulus, cm.

F_c = frictional force on the cylindrical portion of the body, g.-force

F_g = gravitational force on the falling body, g.-force

F_{ee} = frictional force due to the entrance-exit effect, g.-force

F_{st} = frictional force due to the stabilizers, g.-force

$f = 4F_g g_c\,D_e/\pi\,D_1^2\,\rho\,v^2 l$ = total friction factor, dimensionless

f_c = cylinder friction factor pertaining to F_c, dimensionless

f_{ee} = entrance-exit friction factor pertaining to F_{ee}, dimensionless

f_{st} = stabilizer friction factor pertaining to F_{st}, g.-force-cm./g.-mass-(sec.^{2})

g = local acceleration of gravity, cm./sec.^{2}

g_c = gravitational conversion constant, g.-mass-cm./g.-force-(sec.^{2})

l = length of the cylindrical por-

tion of the viscometer body, cm.

l' = $4V/\pi D_1^2$ = volume equivalent length of the viscometer body, cm.

N_{Re} = $D_e v\rho/\mu$ = Reynolds number, dimensionless

p = pressure, lb./sq. in. gauge

t = temperature, °C.

V = volume of the viscometer body, cc.

v = terminal velocity of the falling body, cm./sec.

Greek Letters

α = temperature coefficient of the viscometer constant, $(°C.)^{-1}$

β = viscometer constant defined by Equation (1), cc./sec.^{2}

β_{isf} = viscometer constant defined by Equation (2), cc./sec.^{2}

$\beta_{(t,p)}$ = viscometer constant of Equation (1) as a function of temperature and pressure, cc./sec.^{2}

$\beta_{(0,0)}$ = viscometer constant of Equation (1) corrected to 0°C. and 1 atm., cc./sec.^{2}

γ = pressure coefficient of the viscometer constant, (lb./sq.in. gauge)$^{-1}$

μ = absolute viscosity, poise or g.-mass/cm.-sec.

ρ = fluid density, g.-mass/cc.

σ = density of the viscometer body, g.-mass/cc.

ϕ = general function

LITERATURE CITED

1. Bridgman, P. W., *Proc. Am. Acad. Arts Sci.*, **61**, 57 (1926).
2. *Ibid.*, **66**, 185 (1931).
3. Hilsenrath, J., et al., *Circular 564*, National Bureau of Standards, Washington, D. C. (1955).
4. Kestin, J., "Transport Properties of Gases," p. 27, Northwestern University Press, Evanston, Illinois (1958).
5. ———, and H. E. Wang, *Physica*, **24**, 694 (1958).
6. Lohrenz, John, Ph.D. thesis, University of Kansas, Lawrence, Kansas (September, 1960).
7. ———, G. W. Swift, and Fred Kurata, *A.I.Ch.E. Journal*, **6**, 547 (1960).
8. Michels, A., and R. O. Gibson, *Proc. Roy. Soc. (London)*, **134A**, 288 (1932).
9. Ross, J. F., and G. M Brown, *Ind. Eng. Chem.*, **49**, 2026 (1957).
10. Rossini, F. D., director, "Selected Values of the Properties of Hydrocarbons and Related Compounds," Carnegie Institute of Technology, Pittsburgh, Pennsylvania (1959).
11. Sage, B. H, and W. N. Lacey, *Ind. Eng. Chem.*, **30**, 829 (1938).
12. Swift, G. W., Ph.D. thesis, University of Kansas, Lawrence, Kansas (June, 1959).
13. ———, John Lohrenz, and Fred Kurata, *A.I.Ch.E. Journal*, **6**, 415 (1960).

Manuscript received March 16, 1961; revision received September 15, 1961; paper accepted September 19, 1961.

The Photochlorination of Chloroform in Continuous Flow Systems

JAMES E. HUFF and CHARLES A. WALKER

Yale University, New Haven, Connecticut

Data on the vapor phase photochlorination of chloroform in flow reactors are interpreted on the basis of reaction mechanisms presented in the literature. In order to estimate the rates of light absorption it is also necessary to interpret the rate data obtained for the uranyl sulfate-oxalic acid reaction.

The chlorination results are represented quite well by a mechanism in which the most important termination step is a termolecular reaction between trichloromethyl radicals and chlorine. Deviations from this model are observed as the flow of reactants becomes turbulent and as the light intensity increases. The observed decrease in reaction rate under such conditions is attributed to the increased significance of a second termination step, the unimolecular deactivation of chlorine radicals at the reactor wall.

Photochemical reactions have been carried out on a commercial scale for many years. It is somewhat surprising then that publications concerning the problem of photoreactor design have begun to appear only recently. The most comprehensive of these recent papers is that of Doede and Walker (*4*). These authors review the fundamentals of photochemical kinetics and show qualitatively how these principles apply to the design of practical photoreactors. No quantitative design relationships are presented in this general paper.

Governale and Clarke (*7*) have presented an interesting history of the development of a commercial photoreactor. The information presented in this paper is largely qualitative, and little is said concerning the application of photochemical and kinetic fundamentals to the problem of scale-up and design.

A more fundamental study of the problem of reactor design was carried out by Baginski (*2*), who studied the addition of hydrogen sulfide to terminal olefins in continuous photoreactors. Unfortunately severe back mixing due to density gradients precluded a detailed interpretation of the results. More recently Gaertner and Kent (*5*) have studied the oxalic acid-uranyl nitrate photolysis in a continuous reactor. These authors rely heavily on physical and kinetic principles in their analysis of the results. However their differential rate equation, though based on classical photochemical laws, is somewhat inconsistent with modern kinetic theory.

An analytical representation of the kinetics of a photoreaction taking place in an isothermal, laminar-flow reactor has been developed by Schechter and Wissler (*11*). Their equations apply only for a reaction first order in light intensity and reactant concentration, and in which the absorbing species is not consumed (photosensitized system). The effect of diffusion and light attenuation on observed over-all conversions are considered in this analysis. No experimental work is presented.

The present study arose from questions regarding the proper methods of application of the theory to the design of photoreactors. It is the purpose of this paper to present data on the vapor-phase photochlorination of chlo-

James E. Huff is with Dow Chemical Co., Midland, Michigan.